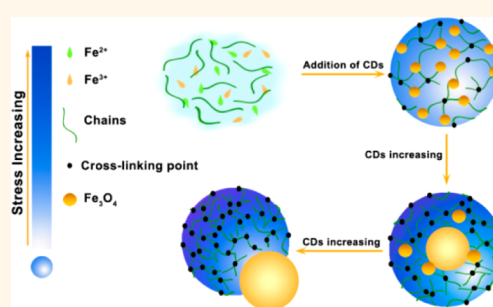


Synthesis of Janus Particles *via* Strain-Driven Microphase Separation and Their Assembly into Nanoscale Vesicles

Wenchao Ding,[†] Yijing Li,[†] Haibing Xia,^{*,†} Dayang Wang,^{*,‡} and Xutang Tao[†]

[†]State Key Laboratory of Crystal Materials, Shandong University, Jinan 250100, P. R. China, and [‡]Ian Wark Research Institute, University of South Australia, Adelaide, South Australia 5095, Australia

ABSTRACT Janus particles, consisting of Fe₃O₄ nanoparticles and organic particles of the complexes of α -cyclodextrin and polyethylene glycol (5) nonylphenyl ether, have been successfully fabricated *via* strain-driven microphase separation, which is distinct from conventional surface wetting-driven microphase separation. The as-prepared Janus particles can self-assemble into hollow spheres, which draw a clear analogy with self-assembly of lipids to vesicles.



KEYWORDS: Janus nanoparticle · strain · microphase separation · lipid · vesicles · self-assembly

In this work, we demonstrate that during formation of organic–inorganic composite particles, proper cross-linking of the organic matrices can induce sufficiently large internal strain, which drives the microphase separation between the organic matrices and newly forming inorganic nanoparticles (NPs) and transforms the homogeneous composite particles to Janus particles. Janus particles are exotic and elegant models to study the complicated organization processes in colloidal science. They have been recognized as advanced building blocks to construct sophisticated supraparticle structures that would not be implemented using isotropic particles.^{1–3} In the past decade, a variety of strategies have been developed to produce Janus particles comprising two chemically distinct domains clearly separated either on the surfaces or in the bulk or both. Microphase separation is one of the very few available strategies enabling reliable and large scale production of colloidally stable Janus particles. This strategy was initially developed to produce Janus polymer particles.⁴ Now it is applied to preparation of inorganic/polymer or inorganic/inorganic

Janus particles^{2,3} based on microphase separation either within emulsion droplets⁵ or on the surfaces of preformed particles.⁶

Current microphase separation strategies rely predominantly on the incompatibility between two constituent components embodied in the bulk phases of target particles or between two stabilizing ligands on the particle surfaces.^{2,3} The final particle structures from partial (core@shell and Janus type) to complete phase-separation (nonengulfing) are determined by the balance of the interfacial tensions between three phases, two constituent solid phases and one solvent phase, embodied in the reaction systems.⁷ In many systems, particularly in the presence of stabilizing ligands, however, the large surface energy contrast between two separated phases with different chemical nature may be significantly smeared out by the ligands stabilizing either or both of these two phases, leading to homogeneous mixing of the two phases at least on the nanoscale and thus yielding homogeneous composite particles.

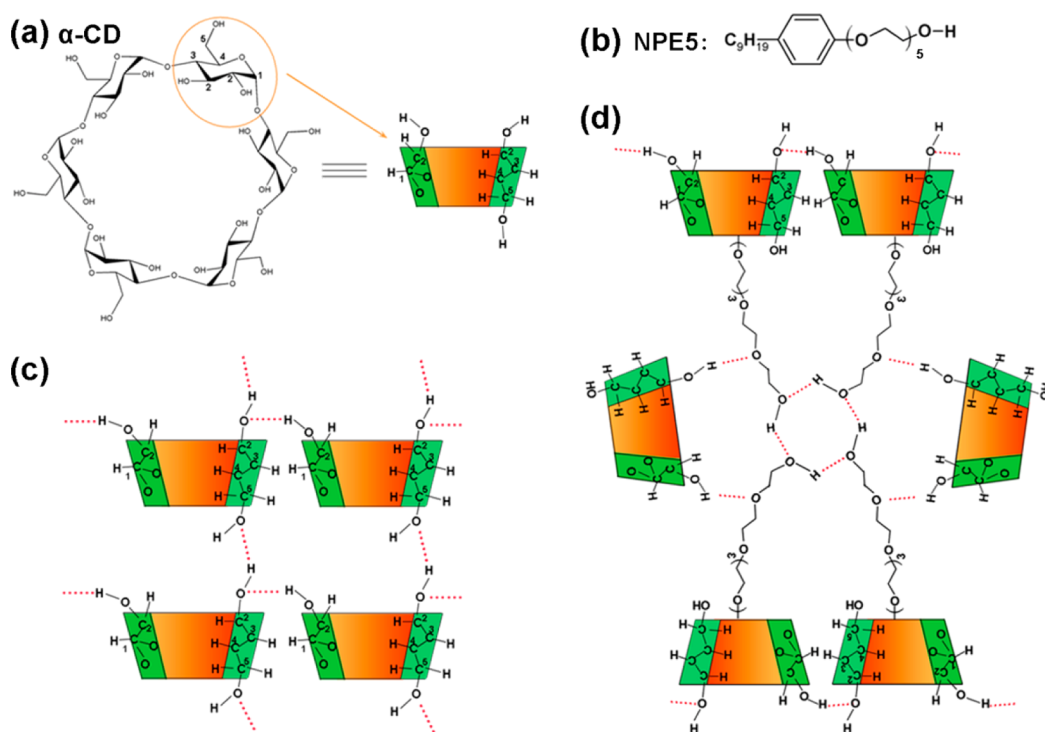
Hydrogen bonding is one of the important interactions involved in determining the three-dimensional structures of proteins,

* Address correspondence to hbxia@sdu.edu.cn, Dayang.Wang@unisa.edu.au.

Received for review June 23, 2014 and accepted October 23, 2014.

Published online October 23, 2014 10.1021/nn503382v

© 2014 American Chemical Society



Scheme 1. Molecular structure of α -CD (a) and NPE5 (b), possible hydrogen bonds formed among α -CDs (c), and between α -CDs and NPE5 (d).

nucleic acids, or carbohydrates. It is also used to control the type and shapes of the nanoparticle clusters. For example, it was reported by the Rotello group⁸ that polymeric layer protected gold particles self-assembled into spherical aggregates through hydrogen-bonding interactions. In their strategy, the polymers acted as the mortar to hold the colloidal particles together to form spherical aggregates. It was also reported in our previous work⁹ that the hydroxyl groups of the α -cyclodextrin (α -CD) rims can interact with the hydrophilic moiety of the surfactant and the CDs after the formation of an inclusion complex with the hydrophobic groups of the surfactant NPE n (where $n = 5, 9, \text{ or } 30$). This would result in the possible formation of hydrogen bonds between α -CDs, and between the surfactant NPE n and α -CDs^{10–13} (Scheme 1). First, linear NPE5-CD complexes are quickly formed due to the host–guest relation. Next, hydrogen bonds between the linear chains of the NPE5-CD complex would be formed by hydroxyl groups from additional CDs. Lastly, a network would be formed due to cross-linking between linear NPE5-CD complexes. As the number of hydrophilic groups of the surfactant NPE n and α -CD concentration increases, it is likely that these interactions among them would increase. This can lead to linkage or bridging of the surface coating on the nanoparticles and further enhance the interactions between singular nanoparticles, causing them to be bound together.⁹ As expected, the morphology of the aggregates of Fe₃O₄ nanoparticles was tuned from mesoporous to hollow and solid when the length of

the hydrophilic groups of the surfactant NPE n was changed from 5 to 9 and 30, respectively. The results indicate that the intensity of hydrogen bonds between the Fe₃O₄ nanoparticles in the aggregates was gradually increased; the intensity of hydrogen bonding is related to the amount of α -CDs and the NPE n .⁹

The hydroxyl groups from α -cyclodextrins have strong adsorption capacity on the surface of Fe₃O₄ nanoparticles, rendering them water-soluble. It has been demonstrated earlier by the Yang group that hydrophobic Fe₃O₄ nanoparticles can be transferred into aqueous solution due to functionalization of Fe₃O₄ nanoparticles with the α -CDs.¹⁴

In our previous work, we mainly focused on the effect of the NPE n surfactants on the aggregates of Fe₃O₄ nanoparticles at the low concentration of α -CDs due to the high cost of α -CDs. To increase the amount of hydrogen bonds, it is easier to increase the concentration of α -CDs, instead of the NPE n surfactants.

In general, a molecule experiences *strain* when its chemical structure undergoes some stress which raises its internal energy in comparison to a strain-free reference compound. Accordingly, the formation of hydrogen bonds among molecules would limit their freedom and induce the internal strain. Herein we demonstrate that cross-linking of host matrices can induce sufficiently strong internal strain to squeeze newly formed guest NPs out of the host matrices with increasing amount of hydrogen bonds formed among NPE5, CDs and NPE5-CD complexes. In addition, the distribution of strain is localized due to the

gradual addition of CDs, instead of addition in a lump. Here this strain-driven microphase separation concept has successfully led to colloidal Janus particles consisting of 10 ± 1 nm Fe_3O_4 NPs and 22 ± 2 nm organic particles of the complexes (α -CD-NPE5) of α -cyclodextrin (α -CDs) and polyethylene glycol (5) nonylphenyl ether (NPE5). However, such Janus NPs cannot be obtained when NPE9 or NPE30 is used, which should occur because the number of hydrogen bonds between CDs and NPE5 can be tuned with increasing concentrations of CD, while those between CDs and NPE9 (or NPE30) are too strong to be tunable. Note that since their surfaces are coated with the α -CD-NPE5 complexes, the Fe_3O_4 NPs can be well dispersed within the α -CD-NPE5 complex particles when the complex particles are weakly cross-linked. As-prepared $\text{Fe}_3\text{O}_4/\alpha$ -CD-NPE5 Janus particles exhibit excellent colloidal stability in water and can readily self-assemble into hollow spheres composed of double layers of the Janus particles, reminiscent of lipid vesicles, upon adding ethanol into the aqueous dispersion of Janus particles. Up to date, colloidal magnetic particles or Janus particles with magnetic parts have been successfully guided to self-assemble into linear or zigzag chains or circular dipolar structures especially under zero magnetic field.^{15–24} The success of directing magnetic particles to more complicated architectures like vesicles by self-assembly is rarely reported.

RESULTS AND DISCUSSION

In our work, Fe_3O_4 NPs were synthesized in the presence of both NPE5 and α -CD *via* the conventional co-precipitation method in water. First, Fe^{2+} and Fe^{3+} ions were added into the aqueous solution of NPE5 ligands under constant stirring and nitrogen protection. Into the resulting solution was the α -CD/ammonia mixture added dropwise for about 30 min, followed by 24 h incubation. As such, Fe_3O_4 NPs were expected to be formed and stabilized with the α -CD molecules anchored on their surfaces,¹⁴ while the NPE5 molecules were expected to form complexes with the α -CD molecules due to the strong inclusion of either the nonylphenyl or poly(ethylene glycol) moieties of the NPE5 molecules or both in the cavities of the α -CD molecules.²⁵ Taking into account that all these processes occur simultaneously, the α -CD-NPE5 complexes and the α -CD-stabilized Fe_3O_4 NPs are expected to be cross-linked (Scheme 1) to form organic/inorganic composite particles. In the current work, the amounts of Fe^{2+} ions, Fe^{3+} ions, ammonia, and NPE5 were fixed, while the amount of α -CD added was adjusted to alter the final structures of as-prepared composite particles by tuning the cross-linking degree due to the formation of different amount of hydrogen bonds, which were visualized by transmission electron microscopy (TEM). As shown in Figure 1, when the α -CD-to-NPE5 molar ratio is adjusted around 12.5,

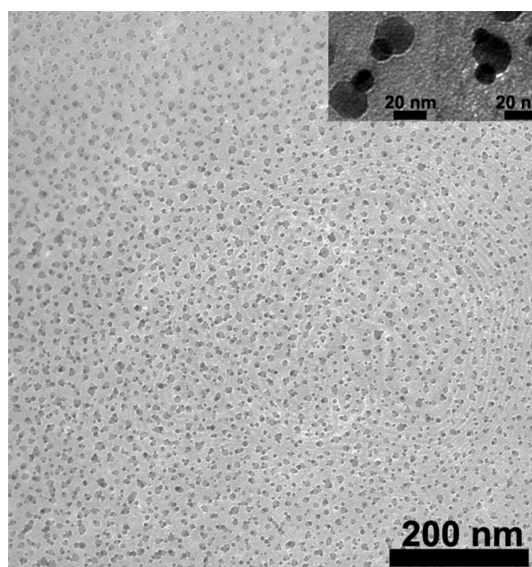


Figure 1. TEM image of $\text{Fe}_3\text{O}_4/\alpha$ -CD-NPE5 Janus particles obtained *via* addition of ammonia/ α -CD mixtures to aqueous solution of $\text{Fe}^{2+}/\text{Fe}^{3+}/\text{NPE5}$ mixtures. The concentrations of Fe^{2+} ions, Fe^{3+} ions, ammonia, NPE5, and α -CD are 0.010 M, 0.020 M, 240 mM, 0.72 mM, and 9.0 mM, respectively. The α -CD-to-NPE5 molar ratio is 12.5. The insets show the high magnification TEM images of as-prepared Janus particles bearing one (left panel) and two Fe_3O_4 NPs (right panel) in one α -CD-NPE5 complex domain, respectively.

Janus particles, which consist of one relatively spherical dark domain with sizes in the range of 22 ± 2 nm and one uniform black dot with sizes of 10 ± 1 nm, are produced at high production yield. Due to the clear imaging contrast, the dark domains can be assigned to the organic phases of α -CD-NPE5 complexes and the black dots to the inorganic phases of Fe_3O_4 NPs (inset of the left panel on the upper right corner in Figure 1), respectively. The chemical composition of as-prepared Janus particles was also verified by the selected area diffraction pattern (Supporting Information Figure S1) and the FTIR spectrum (Supporting Information Figure S2). The Fe_3O_4 nature of the resulting iron oxide NPs was further confirmed by Mössbauer spectroscopy (Supporting Information Figure S3). Careful assessment of TEM images indicates that about 20% of as-prepared Janus NPs contain two or even three Fe_3O_4 NPs decorated on one α -CD-NPE5 complex domain (Inset of the right panel on the upper right corner in Figure 1).

When the α -CD/ammonia mixture is added into the aqueous solution of $\text{NPE5}/\text{Fe}^{2+}/\text{Fe}^{3+}$ mixtures, α -CD molecules are expected to immediately form complexes with NPE5 molecules *via* strong host–guest inclusion interaction. The α -CD-NPE5 complexes are subsequently cross-linked *via* hydrogen bonds between the hydroxyl groups on the α -CD exterior surfaces of either neighboring parts of the complexes or between the complexes and excess α -CD molecules (Scheme 1).

In parallel to complexation with NPE5 molecules, α -CD molecules are also expected to stabilize newly

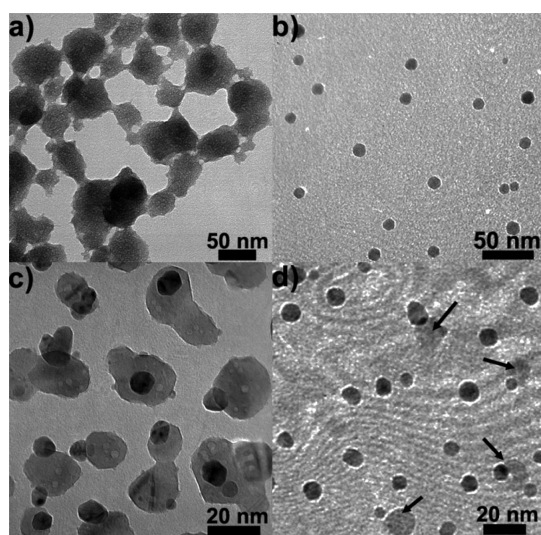


Figure 2. TEM image of $\text{Fe}_3\text{O}_4/\alpha\text{-CD-NPE5}$ Janus particles obtained *via* addition of ammonia/ $\alpha\text{-CD}$ mixtures to the aqueous solution of $\text{Fe}^{2+}/\text{Fe}^{3+}/\text{NPE5}$ mixtures. The concentrations of Fe^{2+} ions, Fe^{3+} ions, ammonia, and NPE5 are 0.010 M, 0.020 M, 240 mM, and 0.72 mM, respectively. The concentration of $\alpha\text{-CD}$ is varied from 1.80 to 12.2 mM, corresponding to an $\alpha\text{-CD}$ -to-NPE5 molar ratio of 2.5 (a), 7.0 (b), 14 (c), and 17 (d). In panel d, the spheres of $\alpha\text{-CD-NPE5}$ complex are indicated by black arrows.

formed Fe_3O_4 NPs by anchoring their exterior surface hydroxyl groups on the NP surfaces, which make the Fe_3O_4 NPs well dispersed within the $\alpha\text{-CD-NPE5}$ complex matrices. Thus, the incompatibility between the different phases embodied in $\text{Fe}_3\text{O}_4/\alpha\text{-CD-NPE5}$ composite particles is expected to be not sufficiently large to guide the formation of the Janus structures.

To reveal the mechanism behind the formation of $\text{Fe}_3\text{O}_4/\alpha\text{-CD-NPE5}$ Janus particles, we investigated how the structures of the $\text{Fe}_3\text{O}_4/\alpha\text{-CD-NPE5}$ composite particles are correlated with the $\alpha\text{-CD}$ -to-NPE5 molar ratio (Figure 2). When the $\alpha\text{-CD}$ -to-NPE5 molar ratio is at 2.5 or below, round composite clumps are obtained, in which tiny Fe_3O_4 NPs of 3–4 nm in size are homogeneously inlaid in the $\alpha\text{-CD-NPE5}$ complex matrices and tend to agglomerate (Figure 2a) as NPE5 plays a key role at low concentration of $\alpha\text{-CD}$ s. The result is also in good agreement with our previous results.⁹ With $\alpha\text{-CD}$ -to-NPE5 molar ratio increasing to about 5, Fe_3O_4 NPs with sizes of *ca.* 10 nm are obtained and enclosed by thin $\alpha\text{-CD-NPE5}$ complex shells which cannot be directly observed due to the low contrast (Figure 2b). The shell thickness of the $\alpha\text{-CD-NPE5}$ complex becomes noticeable when the $\alpha\text{-CD}$ -to-NPE5 molar ratio is in the range of 7–10 (Supporting Information Figure S4), highlighting the clear separation between the Fe_3O_4 NP phase and the $\alpha\text{-CD-NPE5}$ complex phase. When the $\alpha\text{-CD}$ -to-NPE5 molar ratio is in the range of 10–14, fairly uniform Janus particles, as shown in Figure 1, are obtained. When the $\alpha\text{-CD}$ -to-NPE5 molar ratio is larger than 14, irregular microphase separation structures are observed, where Fe_3O_4 NPs

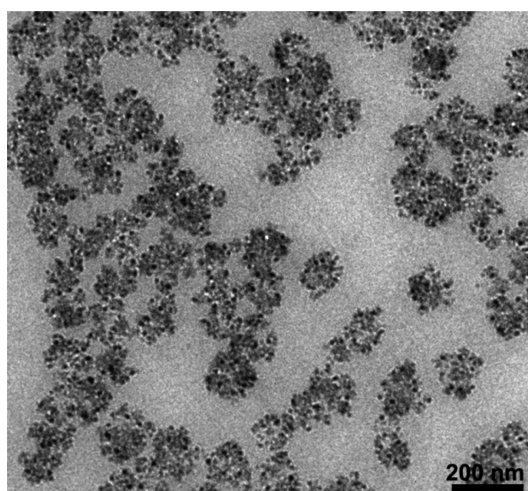
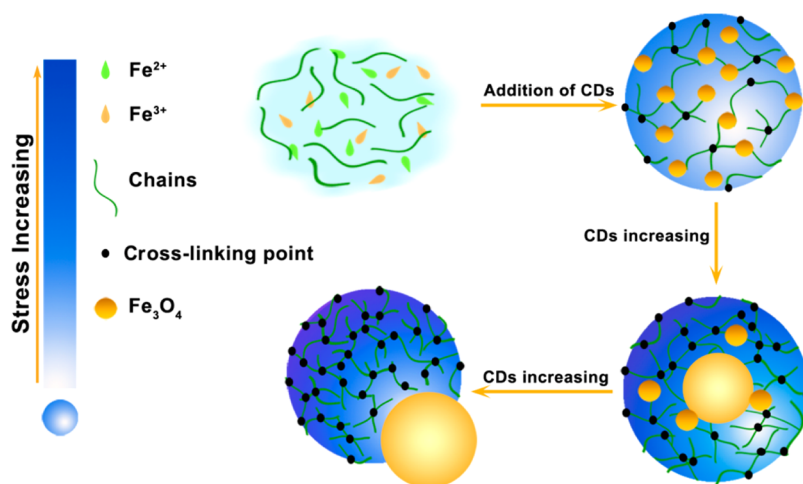


Figure 3. TEM image of the intermediate product extracted from reaction solution during the formation of Janus particles. The concentrations of Fe^{2+} ions, Fe^{3+} ions, ammonia, NPE5, and $\alpha\text{-CD}$ are 0.010 M, 0.020 M, 240 mM, 0.72 mM, and 9.0 mM, respectively. The $\alpha\text{-CD}$ -to-NPE5 molar ratio is 12.5.

with sizes of about 10 nm are randomly located within irregular particles of $\alpha\text{-CD-NPE5}$ complexes (Figure 2c). Further increase of the $\alpha\text{-CD}$ -to-NPE5 molar ratio above 17 leads to complete separation of 10 nm Fe_3O_4 NPs from spheres of $\alpha\text{-CD-NPE5}$ complex (Figure 2d). These results underline a critical role of the $\alpha\text{-CD}$ -to-NPE5 molar ratio during formation of $\text{Fe}_3\text{O}_4/\alpha\text{-CD-NPE5}$ Janus particles. Note that Fe_3O_4 NPs in all microphase separated nanostructures obtained at $\alpha\text{-CD}$ -to-NPE5 molar ratios in the range of 5–17, have fairly similar sizes, *ca.* 10 nm, which is reasonable as the amounts of Fe^{2+} ions, Fe^{3+} ions, NPE5 and ammonia are kept constant in all experiments.

The $\alpha\text{-CD}$ -to-NPE5 molar ratio is expected to gradually rise from zero to the target value with the time of adding $\alpha\text{-CD}$ /ammonia mixtures into $\text{Fe}^{2+}/\text{Fe}^{3+}/\text{NPE5}$ mixtures. Upon addition of an $\alpha\text{-CD}$ /ammonia mixture, Fe_3O_4 NPs and $\alpha\text{-CD-NPE5}$ complexes are expected to be simultaneously formed. The Fe_3O_4 NPs are stabilized mainly by either $\alpha\text{-CD}$ molecules or $\alpha\text{-CD-NPE5}$ complexes or both *via* the hydroxyl groups of the $\alpha\text{-CD}$ rims anchored on the NP surfaces. The $\alpha\text{-CD-NPE5}$ complexes are also expected to be cross-linked *via* hydrogen bonding of the hydroxyl groups of $\alpha\text{-CD}$ exterior surfaces of either neighboring parts of the complexes or between the complexes and excess $\alpha\text{-CD}$ molecules (Scheme 1). In the later scenario, since the $\alpha\text{-CD}$ molecules anchored on the surfaces of coated Fe_3O_4 NPs still have hydroxyl groups available on their rims, $\alpha\text{-CD}$ -coated Fe_3O_4 NPs are expected to act like excess $\alpha\text{-CD}$ s and are inlaid within the newly growing particles of $\alpha\text{-CD-NPE5}$ complexes, leading to $\text{Fe}_3\text{O}_4/\alpha\text{-CD-NPE5}$ composite particles. As shown in Figure 3, Fe_3O_4 NPs were formed in the shrinking matrices made of the $\alpha\text{-CD-NPE5}$ complex. These Fe_3O_4 NPs may serve as weaker cross-linkers as they are movable, which can



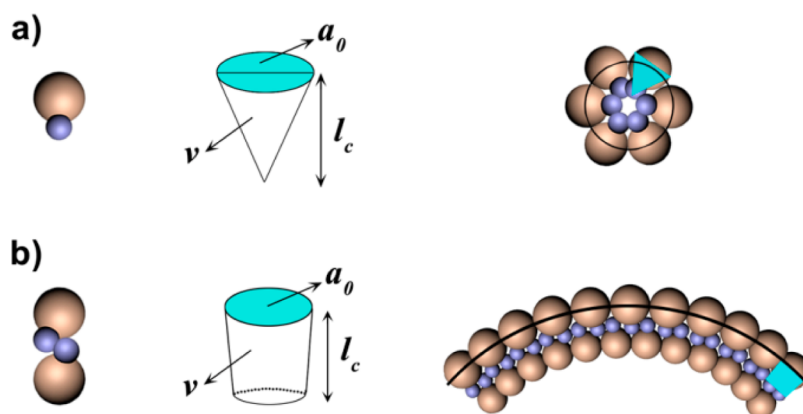
Scheme 2. Schematic depiction of strain-driven microphase separation within $\text{Fe}_3\text{O}_4/\alpha\text{-CD-NPE5}$ complex particles during addition of $\alpha\text{-CD}$ /ammonia mixtures to $\text{Fe}^{2+}/\text{Fe}^{3+}/\text{NPE5}$ mixtures.

be demonstrated by the presence of empty holes in the particles of $\alpha\text{-CD-NPE5}$ (Figure 2c). The possible strain-driven microphase separation process within $\text{Fe}_3\text{O}_4/\alpha\text{-CD-NPE5}$ complex particles is depicted in Scheme 2.

These NPE5 molecules can form micelles or vesicles in water, which may provide a template for the nucleation of Fe_3O_4 nanoparticles. NPE5 actually stabilizes the nanoparticles in the initial stage due to the low amount of CDs. When the amount of $\alpha\text{-CD}$ is increased, these protection layers of NPE5 are reduced due to the formation of $\alpha\text{-CD-NPE5}$ complexes. At fixed NPE5 concentration, the shell thickness in the core@shell Fe_3O_4 NPs can be increased with increasing CD concentration (Figure 2b and Supporting Information Figure S2). However, strain in the organic phase gradually generated locally due to the gradual addition of CDs. Accordingly, the whole particles would release the internal strain by ejecting the big Fe_3O_4 nanoparticles. The process leads to the gradual ejection of Fe_3O_4 particles from organic matrices of $\alpha\text{-CD-NPE5}$ complexes. However, in the absence of NPE5, only Fe_3O_4 nanoparticles with sizes of about 5 nm were obtained (Supporting Information Figure S5), which are stabilized by CDs and can be stable in the solution. These Fe_3O_4 nanoparticles with CDs alone would agglomerate and precipitate due to strong magnetic dipolar interactions, but can be redispersed into the solution (Supporting Information Movie S1). The result also indicates that the $\alpha\text{-CDs}$ have stronger affinity to Fe_3O_4 nanoparticles and limit their size to 5 nm. On the other side, aggregates of $\alpha\text{-CD-NPE5}$ complexes were still obtained in the absence of Fe_3O_4 nanoparticles (Supporting Information Figure S6).

According to its molecular structure (Scheme 1b), each NPE5 molecule needs 1 $\alpha\text{-CD}$ molecule to include its hydrophobic nonylphenyl moiety and maximum 3 $\alpha\text{-CD}$ molecules to include its hydrophilic poly(ethylene glycol) (5) moiety.²⁵ Thus, full formation of

linear NPE5-CD complexes needs about 4 units. In addition, CDs have to stabilize Fe_3O_4 nanoparticles due to strong affinity. Furthermore, more CDs are also necessary for formation of strong networks by formation of more hydrogen bonds formed between linear NPE5-CD complexes. When the $\alpha\text{-CD-to-NPE5}$ molar ratio is less than 4 (e.g., 2.5), the amount of $\alpha\text{-CD}$ molecules should be insufficient to stabilize newly formed Fe_3O_4 NPs and even include the hydrophobic nonylphenyl moieties of all NPE5 molecules due to competition between NPE5 inclusion and the NP surface adsorption, thus leading to large clumps (Figure 2a). When more $\alpha\text{-CD}$ molecules are added to increase the $\alpha\text{-CD-to-NPE5}$ molar ratio above 4, the numbers of $\alpha\text{-CD}$ molecules added should be sufficient to include the hydrophobic nonylphenyl moieties of all NPE5 molecules to form 1-to-1 $\alpha\text{-CD-NPE5}$ complexes. In this case, although free $\alpha\text{-CD}$ molecules are still not sufficient to stabilize newly formed Fe_3O_4 NPs, the $\alpha\text{-CD-NPE5}$ complexes can adsorb onto the NPs to facilitate the NP stabilization, which enable the Fe_3O_4 NPs to grow bigger, thus yielding core@shell structured $\text{Fe}_3\text{O}_4@\alpha\text{-CD-NPE5}$ particles (Figure 2b and Supporting Information Figure S2). With more $\alpha\text{-CD}$ molecules added into the reaction systems, additional free $\alpha\text{-CD}$ molecules can not only include the NPE5 hydrophilic poly(ethylene glycol) (5) moieties of the as-prepared $\alpha\text{-CD-NPE5}$ complex, either dissolved in reaction media or adsorbed on Fe_3O_4 NPs, but also be integrated as cross-linkers into the $\alpha\text{-CD-NPE5}$ complex shells on the NPs to increase both the shell thickness and cross-linking degree. The latter makes the $\alpha\text{-CD-NPE5}$ complex shells more rigid, thus enlarging the internal strain within the shells. With more $\alpha\text{-CD}$ molecules integrated into the $\alpha\text{-CD-NPE5}$ complex shells on the Fe_3O_4 NPs, *i.e.*, the increase of $\alpha\text{-CD-to-NPE5}$ molar ratio, the strain eventually becomes sufficiently strong to drive the increasingly rigid shells of $\alpha\text{-CD-NPE5}$ complexes to crack and in turn squeeze out the



Scheme 3. Geometric model and effective shape of Janus particles and the corresponding preferential aggregation configurations: spheres (a) and vesicles (b). To achieve a clear view to illustrate the aggregation configurations, the head of Janus NPs in the inner part was drawn smaller than that in the outer part.

Fe_3O_4 NPs. On the other hand, this strain is to a small or large degree offset by the hydrogen bonding of the hydroxyl groups on the α -CD rims between the α -CD-NPE5 complex shells and the α -CD molecules (as well as α -CD-NPE5 complexes) directly anchored on the Fe_3O_4 NP cores, which slows down the core@shell separation, thus enabling formation of Janus type structures at a proper range of α -CD-to-NPE5 molar ratio (Figure 1). With more α -CD molecules added to further increase the cross-linking degree and in turn the internal strain of the α -CD-NPE5 complex parts, organic and inorganic phases are eventually completely separated from each other (Figure 2d). As depicted in Scheme 2, therefore, the microphase separation of $\text{Fe}_3\text{O}_4/\alpha$ -CD-NPE5 composite particles is driven by the internal stress arising from the increasing cross-linking degree due to increasing α -CD-to-NPE5 molar ratios. The current results are also in good agreement with recent work²⁶ that the increasing internal interactions would lead to the formation of spherical shape of an organic phase to reduce the surface to volume ratio (S/V).

Conventional incompatibility-driven microphase separation should be a thermodynamically controlled process;⁷ the reaction kinetics may affect the production yield and the dimensions of Janus particles. In contrast, we found that the successful formation of well-defined $\text{Fe}_3\text{O}_4/\alpha$ -CD-NPE5 Janus particles was dependent strongly on the reaction kinetics. Janus particles could be produced at the α -CD-to-NPE5 molar ratio of 12.5 only if the time of addition of α -CD/ammonia mixtures into NPE5/ $\text{Fe}^{2+}/\text{Fe}^{3+}$ mixtures was longer than 30 min. This underlines the kinetic-controlled character of the present strain-driven microphase separation. Our ensuing research focuses on study of the kinetics of adding α -CD/ammonia mixtures into $\text{Fe}^{2+}/\text{Fe}^{3+}/\text{NPE5}$ mixtures at the α -CD-to-NPE5 molar ratio in the range of 12.5–17.5 to manipulate the dimension and microphase separation degree of as-prepared $\text{Fe}_3\text{O}_4/\alpha$ -CD-NPE5 Janus particles.

From the point of view of morphology, Janus particles are regarded as nanoscale analogues of surfactants and envisaged to agglomerate in a way fairly similar to that of surfactants.²⁷ Different from surfactants consisted with clearly separated hydrophobic and hydrophilic parts, as-prepared $\text{Fe}_3\text{O}_4/\alpha$ -CD-NPE5 Janus particles are colloiddally stable in water and the surface coatings of their Fe_3O_4 NP parts and the α -CD-NPE5 complex parts are expected identically hydrophilic due to α -CD coating. Thus, we added a poor solvent for α -CD molecules—ethanol—into the aqueous dispersions of the Janus particles to trigger the particle aggregation. For surfactant aggregates, their morphology is usually determined by the volume of the hydrocarbon part (V), the chain length of their extended all-trans alkyl tails, and the mean headgroup cross-sectional (effective) surface area (a_0) of surfactants, which can be represented by the packing parameter (P), as estimated by $P = V/a_0l_c$.²⁸ Surfactants self-assemble into spherical micelles when $P < 1/3$. For $\text{Fe}_3\text{O}_4/\alpha$ -CD-NPE5 Janus particles shown in Figure 1, their P is calculated to 0.21 (Scheme 3a).

Figure 4a shows that $\text{Fe}_3\text{O}_4/\alpha$ -CD-NPE5 Janus particles do not agglomerate into micelle-like (spherical) aggregates but into hollow spherical aggregates with diameters in the range of 140–170 nm and shell thickness of about 40–50 nm. To further determine the arrangement of Fe_3O_4 NPs in the shells of hollow spherical aggregates, we utilized as-prepared hollow spherical aggregates as templates to form hollow silica spheres. After removal of the organic components by calcination, the hollow spherical shells were composed of single layers of Fe_3O_4 NPs (Figure 5). These results suggest that the resulting hollow spherical aggregates are composed of $\text{Fe}_3\text{O}_4/\alpha$ -CD-NPE5 Janus particles agglomerating in an alternatively up and down ordering fashion, reminiscent of vesicles (Figure 4c and Scheme 3b).

Why do $\text{Fe}_3\text{O}_4/\alpha$ -CD-NPE5 Janus particles prefer to self-assemble into vesicle-like rather than micelle-like

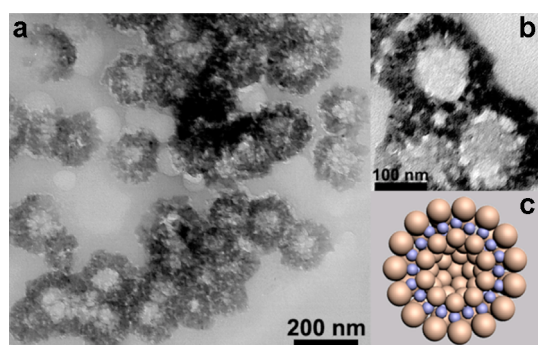


Figure 4. (a) Low and (b) high magnification TEM images and geometrical model (c) of the vesicle-like aggregates obtained via self-assembly of $\text{Fe}_3\text{O}_4/\alpha\text{-CD-NPE5}$ Janus particles induced by addition of a trace amount of ethanol.

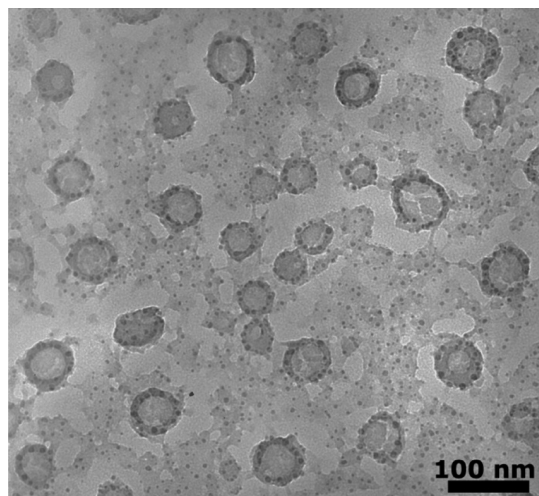


Figure 5. TEM image of hollow silica spheres obtained by using hollow aggregates of $\text{Fe}_3\text{O}_4/\alpha\text{-CD-NPE5}$ Janus particles as templates for sol-gel reactions of tetraethyl orthosilicate (TEOS), followed by calcination to remove the organic components.

structures? First, Janus particles are obviously much larger than surfactant molecules and their constituent parts are more rigid and less flexible than the hydrophobic tails and hydrophilic heads of surfactants to change their morphologies to adapt to dense packing structures. From a steric hindrance point of view, therefore, it is difficult for Janus particles to self-assemble into densely packed micelle-like aggregates. Second, according to literature,^{17,19} Janus particles

tend to agglomerate alternatively up and down to maximize the packing density. When $\text{Fe}_3\text{O}_4/\alpha\text{-CD-NPE5}$ Janus particles agglomerate in an alternating up and down manner (Scheme 3b), their P -values are calculated to be 0.83. It is known that surfactants with P in the range of 0.5–1, for instance lipids, tend to self-assemble into vesicles. Third, the hydrogen bonding between $\alpha\text{-CD}$ rim hydroxyl groups is known to be very strong.^{9–13} Strong attractive interparticle forces are known to promote fast and strong agglomeration of particles into two-dimensional sheets.^{29–31} For self-assembly of lipids into vesicles, lipid bilayers are expected to coalesce to a critical dimension to become properly elastic to fold into cap-like structures and, at the same time, to maintain the cap-like structure stable and to avoid collapse.²⁹ This proper elasticity is usually hardly implemented for self-assembly of hard particles, including Janus particles consisting of two hard constituent parts. In our case, the $\alpha\text{-CD-NPE5}$ complex parts of as-prepared Janus particles, albeit being largely cross-linked, can be regarded as gel particles, which can provide elasticity for the sheets of $\text{Fe}_3\text{O}_4/\alpha\text{-CD-NPE5}$ Janus particles to bend into hollow spheres.

CONCLUSIONS

In summary, we demonstrate a new strategy of strain-induced microphase separation to create organic/inorganic Janus particles. Our approach can be more generally adopted for large-scale production of Janus particles as it does not necessarily rely on the incompatibility or large surface energy contrast between two constituent components, which is necessitated in conventional microphase separation strategies. As-prepared $\text{Fe}_3\text{O}_4/\alpha\text{-CD-NPE5}$ Janus particles can readily self-assemble into hollow spheres upon addition of ethanol. The way in which the Janus particles self-assemble is very similar to that of lipids to vesicles. To our best knowledge, as-prepared $\text{Fe}_3\text{O}_4/\alpha\text{-CD-NPE5}$ Janus particles should provide the first nanoscale analogue of lipids. They and their vesicle-like assemblies may provide not only interesting models to study the self-assembly behavior of synthetic and biological lipids but also new building blocks to be applied directly and indirectly as templates to create new vehicles for drug encapsulation and delivery.

METHODS

Chemicals. Polyethylene glycol(5) nonylphenyl ether (NPE5), iron(II) chloride tetrahydrate ($\text{FeCl}_2 \cdot 4\text{H}_2\text{O}$), and anhydrous iron(III) chloride (FeCl_3) were purchased from Sinopharm Chemical Reagent Co. and Ltd; α -cyclodextrin ($\alpha\text{-CD}$) was from Fluka (99.9%).

Synthesis of $\text{Fe}_3\text{O}_4/\alpha\text{-CD-NPE5}$ Janus Particles. The aqueous solution of NPE5 (10 wt %, 0.240 g), $\text{FeCl}_2 \cdot 4\text{H}_2\text{O}$ (0.159 g) and FeCl_3 (0.267 g) were consecutively dissolved in 45 mL of water under vigorous mechanical stirring and N_2 protection, followed by 30 min mechanical stirring. Into the resulting mixture solution

was dropwise added the $\alpha\text{-CD}$ /ammonia mixture of the aqueous solutions of ammonia (1.2 mL, 15 M) and $\alpha\text{-CD}$ (30 mL, 12.5 mM). After further vigorous mechanical stirring of the resulting reaction mixtures for 1.5 h, the aqueous suspensions of $\text{Fe}_3\text{O}_4/\alpha\text{-CD-NPE5}$ Janus particles were obtained. The large precipitates in the resulting particle suspensions were filtered out using filter papers.

Self-Assembly of $\text{Fe}_3\text{O}_4/\alpha\text{-CD-NPE5}$ Janus Particles into Vesicles. Ethanol (100 μL) was dropwise added into the aqueous suspension of as-prepared $\text{Fe}_3\text{O}_4/\alpha\text{-CD-NPE5}$ Janus particles (5 mL) under mechanical stirring. The resulting mixture suspensions were

further stirred for 30 min and kept still for 6 h to fully complete the self-assembly of the Janus particles.

Conflict of Interest: The authors declare no competing financial interest.

Supporting Information Available: Selected area diffraction pattern, FTIR spectrum and Mössbauer spectra of as-prepared Fe₃O₄/α-CD-NPE5 Janus particles and additional TEM images. This material is available free of charge via the Internet at <http://pubs.acs.org>.

Acknowledgment. This work is financially supported by Natural Science Foundation of China (51172126, 21473105, 51002086, 51227002 and 51272129), 973 program (2010CB630702) and Shandong Provincial Natural Science Foundation (ZR2010EM006). H.X. is grateful to the Program for New Century Excellent Talents in University (NCET-10-0553), Independent Innovation Foundation of Shandong University (2010JQ013) and Scientific Research Foundation for the Returned Overseas Chinese Scholars, State Education Ministry for the financial support. D.W. thanks the Australian Research Council for the financial support (DP 110104179 and DP 120102959).

REFERENCES AND NOTES

- Jiang, S.; Chen, Q.; Tripathy, M.; Luijten, E.; Schweizer, K. S.; Granick, S. Janus Particle Synthesis and Assembly. *Adv. Mater.* **2010**, *22*, 1060–1071.
- Hu, J.; Zhou, S.; Sun, Y.; Fang, X.; Wu, L. Fabrication, Properties and Applications of Janus Particles. *Chem. Soc. Rev.* **2012**, *41*, 4356–4378.
- He, J.; Liu, Y.; Hood, T. C.; Zhang, P.; Gong, J. L.; Nie, Z. H. Asymmetric Organic/Metal(Oxide) Hybrid Nanoparticles: Synthesis and Applications. *Nanoscale* **2013**, *5*, 5151–5166.
- Sheu, H. R.; El-Aasser, M. S.; Vanderhoff, J. W. Phase Separation in Polystyrene Latex Interpenetrating Polymer Networks. *J. Polym. Sci.: Part A: Polym. Chem.* **1990**, *28*, 629–651.
- Torza, S.; Mason, S. G. Three-Phase Interactions in Shear and Electrical Fields. *J. Colloid Interface Sci.* **1970**, *33*, 67–83.
- Chen, T.; Yang, M. X.; Wang, X. J.; Tan, L. H.; Chen, H. Y. Controlled Assembly of Eccentrically Encapsulated Gold Nanoparticles. *J. Am. Chem. Soc.* **2008**, *130*, 11858–11859.
- Chen, Y.; Dimonie, V.; El-Aasser, M. S. Effect of Interfacial Phenomena on the Development of Particle Morphology in a Polymer Latex System. *Macromolecules* **1991**, *24*, 3779–3787.
- Boal, A. K.; Ilhan, F.; Derouchey, J. E.; Thurn-Albrecht, T.; Russell, T. P.; Rotello, V. M. Self-Assembly of Nanoparticles into Structured Spherical and Network Aggregates. *Nature* **2000**, *404*, 746–748.
- Xia, H.; Foo, P.; Yi, J. Water-Dispersible Spherically Hollow Clusters of Magnetic Nanoparticles. *Chem. Mater.* **2009**, *21*, 2442–2451.
- Heyes, S. J.; Clayden, N. J.; Dobson, C. M. ¹³C-CP/MAS NMR Studies of the Cyclomalto-Oligosaccharide (Cyclodextrin) Hydrates. *Carbohydr. Res.* **1992**, *233*, 1–14.
- Cunha-Silva, L.; Teixeira-Dias, J. J. C. Solid State Inclusion of the Nonionic Surfactant C12E4 in α-Cyclodextrin, at Various Humidities: A Combined Raman and ¹³C CP MAS NMR Study. *J. Phys. Chem. B* **2002**, *106*, 3323–3328.
- Rusa, C. C.; Bullions, T. A.; Fox, J.; Porbeni, F. E.; Wang, X.; Tonelli, A. E. Inclusion Compound Formation with a New Columnar Cyclodextrin Host. *Langmuir* **2002**, *18*, 10016–10023.
- Chung, J. W.; Kang, T. J.; Kwak, S.-Y. Guest-Free Self-Assembly of α-Cyclodextrins Leading to Channel-Type Nanofibrils as Mesoporous Framework. *Langmuir* **2007**, *23*, 12366–12370.
- Wang, Y.; Wong, J. F.; Teng, X.; Lin, X. Z.; Yang, H. “Pulling” Nanoparticles into Water: Phase Transfer of Oleic Acid Stabilized Monodisperse Nanoparticles into Aqueous Solutions. *Nano Lett.* **2003**, *3*, 1555–1559.
- Butter, K.; Bomans, P.; Frederik, P.; Vroege, G.; Philipse, A. Direct Observation of Dipolar Chains in Iron Ferrofluids by Cryogenic Electron Microscopy. *Nat. Mater.* **2003**, *2*, 88–91.
- Klokkenburg, M.; Vonk, C.; Claesson, E. M.; Meeldijk, J. D.; Erne, B. H.; Philipse, A. P. Direct Imaging of Zero-Field Dipolar Structures in Colloidal Dispersions of Synthetic Magnetite. *J. Am. Chem. Soc.* **2004**, *126*, 16706–16707.
- Ge, J.; Hu, Y.; Zhang, T.; Yin, Y. Superparamagnetic Composite Colloids with Anisotropic Structures. *J. Am. Chem. Soc.* **2007**, *129*, 8974–8975.
- Hu, M.; Lu, Y.; Zhang, S.; Guo, S.; Lin, B.; Zhang, M.; Yu, S. H. High Yield Synthesis of Bracelet-like Hydrophilic Ni-Co Magnetic Alloy Flux-Closure Nanorings. *J. Am. Chem. Soc.* **2008**, *130*, 11606–11607.
- Zerrouki, D.; Baudry, D.; Pine, D.; Chaikin, P.; Bibette, J. Chiral Colloidal Clusters. *Nature* **2008**, *455*, 380–382.
- Panda, P.; Bong, K. W.; Hatton, T. A.; Doyle, P. S. Branched Networks by Directed Assembly of Shape Anisotropic Magnetic Particles. *Langmuir* **2011**, *27*, 13428–13435.
- Smoukov, S. K.; Gangwal, S.; Marquez, M.; Velev, O. D. Reconfigurable Responsive Structures Assembled from Magnetic Janus Particles. *Soft Matter* **2009**, *5*, 1285–1292.
- Wei, A.; Kasama, T.; Dunin-Borkowski, R. E. Self-Assembly and Flux Closure Studies of Magnetic Nanoparticle Rings. *J. Mater. Chem.* **2011**, *21*, 16686–16693.
- Lattuada, M.; Hatton, T. A. Preparation and Controlled Self-Assembly of Janus Magnetic Nanoparticles. *J. Am. Chem. Soc.* **2007**, *129*, 12878–12879.
- Isajima, T.; Lattuada, M.; Hatton, T. A. Reversible Clustering of pH- and Temperature-Responsive Janus Magnetic Nanoparticles. *ACS Nano* **2008**, *2*, 1799–1806.
- Topchieva, I.; Karezin, K. Self-Assembled Supramolecular Micellar Structures Based on Non-Ionic Surfactants and Cyclodextrins. *J. Colloid Interface Sci.* **1999**, *213*, 29–35.
- Wang, Y.; He, J.; Liu, C.; Chong, W.; Chen, H. Thermodynamics versus Kinetics in Nanosynthesis. *Angew. Chem., Int. Ed.* **2014**, *10.1002/anie.201402986*.
- Mao, Z.; Xu, H.; Wang, D. Molecular Mimetic Self-Assembly of Colloidal Particles. *Adv. Funct. Mater.* **2010**, *20*, 1053–1074.
- Israelachvili, J. N.; Mitchel, D. J.; Ninham, B. W. Theory of Self-Assembly of Hydrocarbon Amphiphiles into Micelles and Bilayers. *J. Chem. Soc., Faraday Trans. 2* **1976**, *72*, 1525–1568.
- Shioi, A.; Hatton, T. A. Model for Formation and Growth of Vesicles in Mixed Anionic/Cationic (SOS/CTAB) Surfactant Systems. *Langmuir* **2002**, *18*, 7341–7348.
- Zhang, B.; Zhao, W. W.; Wang, D. Y. Shape-Controlled Self-Assembly of Colloidal Nanoparticles. *Chem. Sci.* **2012**, *3*, 2252–2256.
- Xia, H.; Su, G.; Wang, D. Size-Dependent Electrostatic Chain Growth of pH-Sensitive Hairy Nanoparticles. *Angew. Chem., Int. Ed.* **2013**, *52*, 3726–3730.